Mapping the Signal-To-Noise-Ratios of Cortical Sources in Magnetoencephalography and Electroencephalography

Daniel M. Goldenholz,[1,2*] Seppo P. Ahlfors,[1,3] Matti S. Hämäläinen,[1,3] Dahlia Sharon,[1] Mamiko Ishitobi,[1] Lucia M. Vaina,[1,2,4] and Steven M. Stufflebeam[1,3]

[1]*Athinoula A. Martinos Center For Biomedical Imaging, Massachusetts General Hospital, Charlestown, Massachusetts*
[2]*Biomedical Engineering Department, Boston University, Boston, Massachusetts*
[3]*Harvard-MIT Division of Health Science and Technology, Massachusetts Institute of Technology, Cambridge, Massachusetts*
[4]*Department of Neurology, Harvard Medical School, Boston, Massachusetts*

Abstract: Although magnetoencephalography (MEG) and electroencephalography (EEG) have been available for decades, their relative merits are still debated. We examined regional differences in signal-to-noise-ratios (SNRs) of cortical sources in MEG and EEG. Data from four subjects were used to simulate focal and extended sources located on the cortical surface reconstructed from high-resolution magnetic resonance images. The SNR maps for MEG and EEG were found to be complementary. The SNR of deep sources was larger in EEG than in MEG, whereas the opposite was typically the case for superficial sources. Overall, the SNR maps were more uniform for EEG than for MEG. When using a noise model based on uniformly distributed random sources on the cortex, the SNR in MEG was found to be underestimated, compared with the maps obtained with noise estimated from actual recorded MEG and EEG data. With extended sources, the total area of cortex in which the SNR was higher in EEG than in MEG was larger than with focal sources. Clinically, SNR maps in a patient explained differential sensitivity of MEG and EEG in detecting epileptic activity. Our results emphasize the benefits of recording MEG and EEG simultaneously. *Hum Brain Mapp 30:1077–1086, 2009.* © 2008 Wiley-Liss, Inc.

Key words: MEG; EEG; epilepsy; forward model; SNR; simulation; dipole; cortex; brain

INTRODUCTION

Although a growing number of clinical methods are available for observing brain activity noninvasively, only two provide millisecond scale temporal resolution with centimeter or better spatial resolution: electroencephalography (EEG) and magnetoencephalography (MEG). Despite being generated by similar neural sources, MEG and EEG signals differ, suggesting that recording both simultaneously is beneficial [Babiloni et al., 2004; Barkley and Baumgartner, 2003; Iwasaki et al., 2005; Knake et al., 2006; Leijten et al., 2003; Lesser, 2004; Lin et al., 2003; Lopes da Silva et al., 1991; Pataraia et al., 2005; Wood et al., 1985; Yoshinaga et al., 2002; Zijlmans et al., 2002]. However, partly

Contract grant sponsor: National Center for Research Resources; Contract grant number: P41RR14074; Contract grant sponsor: NIH; Contract grant numbers: NS37462 and NS44623; Contract grant sponsor: Mental Illness and Neuroscience Discovery (MIND) Institute.

*Correspondence to: Daniel Goldenholz, MGH-Martinos Center, Building 149, 13th St., Charlestown, MA 02129.
E-mail: daniel@nmr.mgh.harvard.edu

Received for publication 13 February 2007; Revised 17 September 2007; Accepted 22 February 2008

DOI: 10.1002/hbm.20571
Published online 8 May 2008 in Wiley InterScience (www.interscience.wiley.com).

© 2008 Wiley-Liss, Inc.

due to the higher cost of an MEG system, neurophysiologists and clinicians are hesitant to adopt the technology, citing studies that conclude the differences in the source localization accuracy between MEG and EEG are minor [Baumgartner 2004; Cohen et al., 1990; Liu et al., 2002]. Conversely, those with experience in MEG often do not record EEG simultaneously, relying on evidence of MEG's more precise localization capabilities [Hämäläinen et al., 1993; Leahy et al., 1998], thereby reducing substantially the pre-recording preparation time required for each subject.

An important potential application of MEG and EEG source localization is the presurgical evaluation of epileptic patients. Epilepsy affects up to 1% of the population in North America [Wiebe et al., 2001]. Approximately 20% of patients do not achieve adequate control of seizures with medication; many of them are candidates for surgery that can reduce or eliminate seizures [Pataraia et al., 2002; Wiebe et al., 2001]. Surgical outcomes are improved by identifying and locating epileptic spikes in MEG and/or in EEG [Ebersole and Pedley, 2002; Stefan et al., 2003]. An epileptic spike must exhibit high enough signal-to-noise-ratio (SNR) to be distinguished from background noise [Cobb, 1983; Iwasaki et al., 2005], and to be localized accurately [Fuchs et al., 1998; Tarkiainen et al., 2003]. The SNR of observed brain activation in EEG and MEG depends not only on the sensor characteristics (type, placement, noise), but also on the location and orientation of the source.

A number of studies have examined sensitivities and expected SNR values of MEG and/or EEG [de Jong et al., 2005; Fuchs et al., 1998; Hillebrand and Barnes, 2002; Tarkiainen et al., 2003]. The present study extends and expands on previous work by incorporating the realistic shape of the cortical surface to impose an anatomical constraint on the locations and orientations of the sources. We examined the difference in SNR between MEG and EEG for each cortical location using both actual noise recordings and a simple noise model to better understand the generalizability of the results. We also compared the SNR of individual dipole sources to that of extended cortical patch sources, and related our findings to the differential detection of epileptic spikes in MEG and EEG.

METHODS

Data Acquisition

Four right-handed subjects (two females), aged 23–42, were included in this study. Each signed a consent form and a privacy statement in accordance with our Institutional Human Subject Research Board and HIPAA standards. High-resolution anatomical magnetic resonance images (MRI) were obtained with a Trio 3T scanner [Siemens Medical Systems, Erlangen, Germany] using MPRAGE pulse sequences (voxel size 1.3 × 1.0 × 1.3 mm^3; slice thickness 1.3 mm; TE 3.31 ms; TR 2530 ms; gap 50%; FOV 10 cm × 10 cm) and FLASH images (flip angle 5°; slice thickness 1.3 mm; FOV 10 cm × 10 cm). MEG and EEG data were acquired simultaneously with a Vectorview™ system [Elekta-Neuromag, Helsinki, Finland] from 204 planar gradiometers, 102 magnetometers, and 70 EEG electrodes (see Fig. 1). Two minutes of spontaneous activity was recorded, sampled at 600 Hz with hardware filters set at 0.1–200 Hz (Subjects 1 and 2) or 0.03–200 Hz (Subjects 3 and 4). The EEG data was transformed to the average electrode reference. Signal-space projection (SSP) was applied to magnetometer data [Tesche et al., 1995] to reduce background environmental noise. The noise subspace for SSP was selected as the three-dimensional space spanned by the eigenvectors corresponding to the three largest eigenvalues of the correlation matrix of a 5-min recording of data collected without a subject present; these correspond approximately to the homogeneous field components, typically originating from environmental (e.g., moving vehicles) sources far from the sensors. The locations of fiducial head points, EEG electrodes, and head-position indicator (HPI) coils were digitized using a FastTrack 3D digitizer [Polhemus, USA]. The location of the MEG sensor array with respect to the head was determined at the beginning of each measurement from the magnetic fields generated by the HPI coils.

The Forward Model

For forward modeling, we used a linear collocation three-layer boundary-element method with conductivity values: 0.3, 0.06, and 0.3 S/m for the brain, skull and scalp, respectively [Hämäläinen and Sarvas, 1989; Hämäläinen et al., 1993]. The surface of the skin, as well as the inner and outer surfaces of the skull were determined from the MRIs (see Fig. 1). Each surface was tessellated with 5120 triangles, providing adequate numerical accuracy [Crouzeix et al., 1999; de Jongh, 2005; Fuchs et al., 2001; Tarkiainen, 2003].

The cortical surface was reconstructed from the MRI data with about 130,000 vertices per hemisphere and an approximate vertex-to-vertex spacing of 1 mm using the Freesurfer software [Dale et al., 1999; Fischl et al., 1999a; Fischl et al., 2001; Segonne et al., 2004]. We computed the MEG and EEG signals predicted by the forward model for dipole sources oriented perpendicular to the gray-white matter boundary at each of the surface vertices.

Neural sources were assumed to be either point sources (current dipoles) or synchronously active patches. For dipolar sources, the source amplitude was 10 nAm; for patches, source strength was chosen to correspond to a uniform surface source density of 50 pAm/mm^2 [Hillebrand and Barnes, 2002; Lu and Williamson, 1991]. To create extended sources, the cortical surface was divided into two complete sets of centroids using the geodesic distance-weighted Dijkstra algorithm [Dijkstra, 1959]. The source patches had geodesic radii of 10 mm or 16 mm, corresponding to areas of 3 cm^2 or 8 cm^2, respectively.

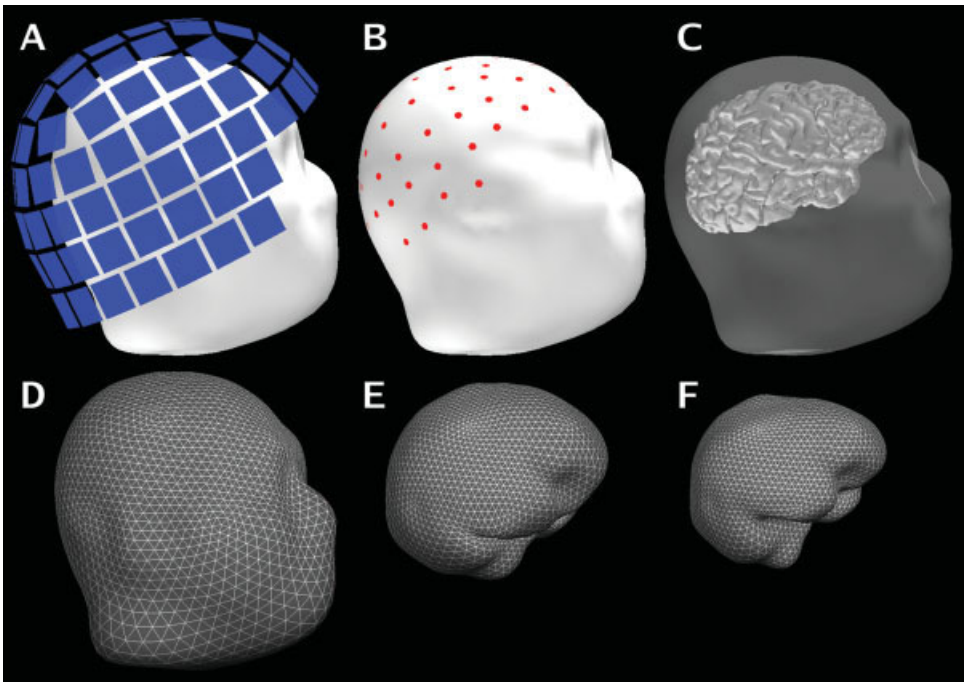

Figure 1.
Sensor and surface configuration. **A**: The locations of the MEG sensor array with respect to the head (Subject 2). **B**: The locations of the EEG electrodes on the scalp. **C**: Surface rendering of the cerebral cortex with the scalp rendered semi-transparent. The second row shows the tessellations of the scalp (**D**), the outer surface of the skull (**E**), and the inner surface of the skull (**F**) employed in the boundary-element forward model. These surfaces were reconstructed from the structural MRI. [Color figure can be viewed in the online issue, which is available at www.interscience.wiley.com.]

Signal-To-Noise Ratio For Individual Sources

We defined the SNR for each source location (dipole or extended patch) in decibel units as:

$$\mathrm{SNR} = 10\log_{10}\left[\frac{a^2}{N}\sum_k \frac{b_k^2}{s_k^2}\right], \quad (1)$$

where b_k is the signal on sensor k provided by the forward model for a source with unit amplitude, a is the source amplitude, N is the number of sensors, and s_k^2 is the noise variance on sensor k.

For the comparison of MEG and EEG, the differential SNR was defined as

$$D = \mathrm{SNR}_{\mathrm{MEG}} - \mathrm{SNR}_{\mathrm{EEG}} \quad (2)$$

Note that D is independent of source amplitude a. If the MEG SNR exceeds that of EEG, then $D > 0$; in the opposite case $D < 0$. For a combined MEG/EEG SNR map, $\max\{\mathrm{SNR}_{\mathrm{MEG}}, \mathrm{SNR}_{\mathrm{EEG}}\}$ was selected at each cortical location. Grand-average SNR maps across the subjects were computed using a spherical morphing procedure that is based on aligning sulcal and gyral features [Fischl et al., 1999b]. The percentage of cortical area where the SNR was higher in MEG than in EEG was determined by computing the fraction of sources for which $D > 0$. Note that under the assumption of additive Gaussian noise, averaging across evoked trials is equivalent to adding a constant to all SNR values in MEG and EEG, and thus will not influence the difference D maps.

Noise Estimation

The noise variance s_k^2 used in the SNR calculations was obtained in two ways. In the first approach, the noise variance $\hat{s}^2_{k,\mathrm{recorded}}$ for each sensor was estimated from MEG and EEG recordings of spontaneous activity, filtered at 0.5–100 Hz. In the second approach, to reduce the influence of idiosyncrasies of the MEG and EEG sensors present during a specific session, we also used an alternative noise model based on uniform background brain activity. The model assumed a uniform spatial distribution of identical independent noise sources [de Munck et al., 1992], oriented perpendicular to the cortical mantle. The amplitudes of the sources were assumed to have a Gaussian distribution with zero mean and variance s_s^2. Since instrumentation noise is typically substantially smaller than signals

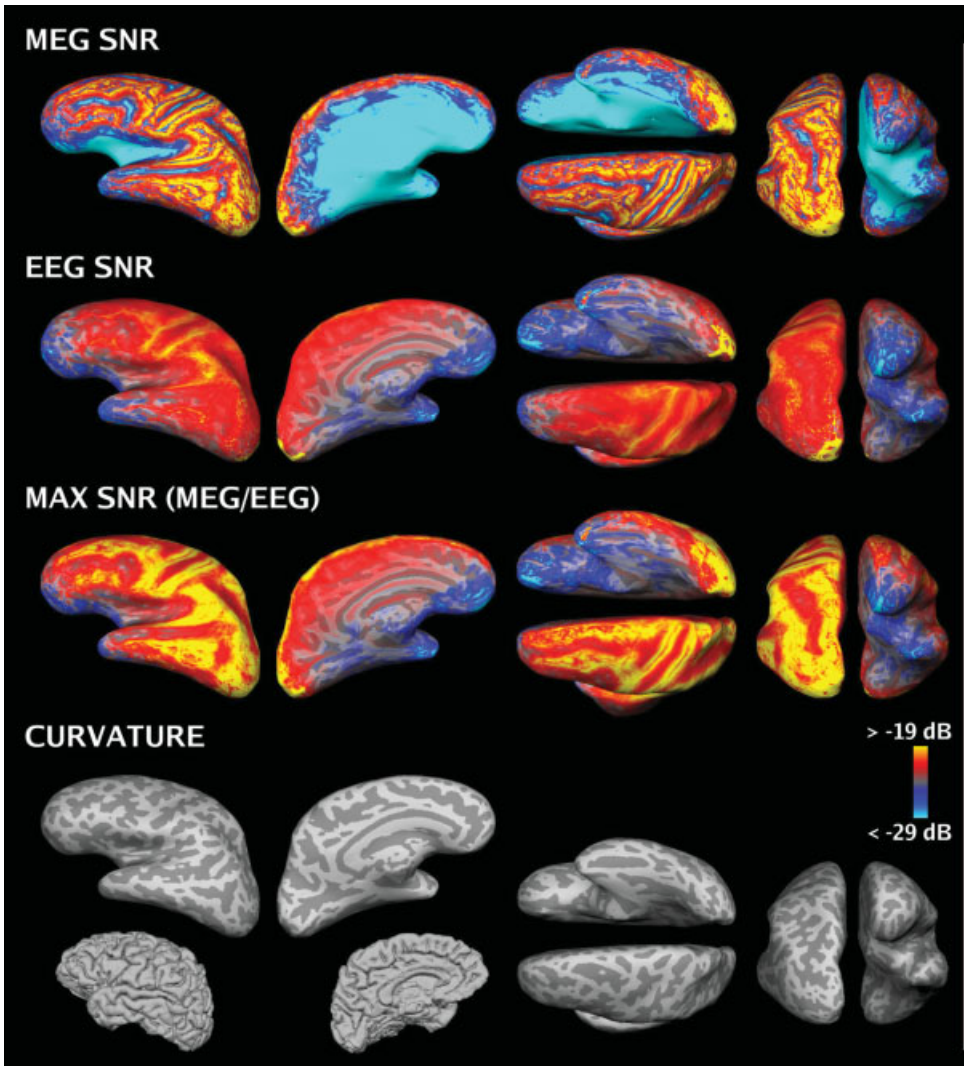

Figure 2.
SNR maps based on the noise model (group average, left hemisphere, plotted on Subject 2's brain). The color scale is identical in each SNR map. The SNR estimates plotted on the cortical surface: SNR_{MEG} (first row), SNR_{EEG} (second row), maximum of SNR_{MEG} and SNR_{EEG} (third row). Fourth row: inflated cortical curvature maps and folded cortex maps. Convex areas (gyri) and concave areas (sulcal walls) are indicated in light and dark gray, respectively.

due to spontaneous brain activity [Ebersole and Pedley, 2002; Hämäläinen et al., 1993], an instrumentation noise term was not included in our model. Under these assumptions, the noise variance for sensor k is

$$s_k^2 = s_s^2(\mathbf{A}\mathbf{A}^T)_{kk}, \quad (3)$$

where $\mathbf{A}$ is the forward solution matrix computed for the noise sources with unit amplitudes, T indicates matrix transpose. For the computation of $\mathbf{A}$, we decimated the dense triangulation of the cortex to an approximate inter-source spacing of 7 mm.

The unknown source variance s_s^2 for the noise model was estimated from the recorded activity $\hat{s}_k^2$. The median values of $\hat{s}_{k,\text{recorded}}^2/(\mathbf{A}\mathbf{A}^\mathbf{T})_{kk}$ were determined separately for the MEG gradiometers, the MEG magnetometers, and the EEG channels. Medians were used to avoid accounting for outlier, or "bad" channels. The mean of the three median values, weighted by the number of channels in each sensor type, was taken as an estimate of s_s^2; these were found to be similar for the four subjects (square root of s_s^2 values: 1.6, 1.6, 1.6, and 1.9 nAm). Thereafter, sensor variances $\hat{s}_k^2$ for MEG and EEG were calculated with Eq. 3 using that overall estimate of the source variance s_s^2.

RESULTS

Signal-To-Noise-Ratio Of Dipole Sources

MEG and EEG SNR maps, averaged over the four subjects, are shown in Figure 2. For MEG, the SNR map showed high SNR on most superficial cortical regions, with lower SNR in deeper areas such as sulci on the lateral surface (in particular, the Sylvian fissure), interhemispheric cortex, and parts of the ventral cortex. The SNR was lowest near the center of the head. In addition, there were thin strips at the crests of gyri with low SNR. These corre-

spond to areas where the source orientations are approximately normal to the nearby surface of the skull. For EEG, the SNR map is much more uniform than that of MEG. The SNR of EEG was low in the inferior frontal areas, probably due to an inadequate sampling of the scalp potential distribution with the present electrode array. The differences between the two modalities suggest that combined recordings can improve the overall SNR of cortical sources (Fig. 2, third row).

A difference SNR map (D map, c.f. Eq. 2) is shown in Figure 3. Deep areas, such as much of the medial surface of each hemisphere and the Sylvian cortex, and the crests of the gyri had a higher SNR in EEG. The frontal and occipital poles had a higher SNR in MEG, as well as most regions on the lateral surface. On the basis of the noise model, the average area (across subjects and hemispheres, excluding the ventricular surfaces) for which SNR was higher in MEG than in EEG was approximately 40% of total area of the cortex.

In Figure 2 and the two top rows of Figure 3, the noise model was used. The bottom row of Figure 3 shows D maps recomputed using variances for each sensor estimated from recorded data. The average area of cortex for which the SNR is higher in MEG than in EEG was 55%, which is somewhat larger than that computed using the noise model. The SNR maps due to recorded noise in MEG and EEG (not shown) suggest that the additional area is due to higher MEG SNR values than predicted by the noise model.

Extended Sources

MEG/EEG signals are likely to arise from extended patches of active cortex [Ebersole and Pedley, 2002]. Figure 4 shows comparison maps generated based on dipoles and extended sources. The value assigned to a source location represents the number of subjects for which $D > 0$ at that point. For many superficial dipolar sources, the MEG SNR was consistently higher in all subjects. This pattern changed with source extent: as the extent increased, the total area of cortex that has higher SNR in MEG became smaller. Nonetheless, several regions had consistently higher SNR in MEG across subjects, including occipital pole, inferior occipital lobe, temporal pole, posterior temporal lobe, and frontal pole.

Clinical Example

To illustrate the practical implications of SNR maps, we present data from an epileptic patient. MEG and EEG were recorded simultaneously from a 38-year-old female with a hypothalamic hamartoma, suffering from intractable complex partial seizures since age 2. We observed frequent epileptic discharges independently from the left and right frontal-temporal regions. We selected two interictal spikes that appeared different in MEG and EEG (see Fig. 5). The first spike (A) was easier to identify in EEG traces, whereas the second spike (B) was easier to identify in MEG traces. Equivalent current dipoles were localized based on the EEG for spike A and on the MEG for spike B. These source locations were then examined using a difference SNR map between MEG and EEG for that patient's cortical anatomy to make *post-hoc* predictions about the SNR. At the obtained dipole locations, the D values based on recorded noise predicted the observed differences between MEG and EEG for both spikes. In contrast, the noise model based D maps (not shown) only predicted SNR difference for spike A. This suggests that the noise model overestimated the MEG noise level for that particular recording session and for that cortical location.

DISCUSSION

We employed realistic cortical geometry models to compare the SNR of cortical sources in EEG and MEG. The SNR maps were found to be complementary, suggesting that the highest overall SNR can be achieved by combined MEG and EEG recordings. Below, we first discuss the effect of various modeling assumptions, including tissue conductivity values, average vs. maximum SNR, number of sensors, and sensor noise estimates. We then consider the relationship between MEG and EEG and the properties of the sources in terms of the SNR maps.

Modeling Assumptions

Our forward model used commonly cited values for tissue conductivities [Hämäläinen et al., 1993]. A recent study [de Jongh et al., 2005] used electrical impedance tomography [Goncalves et al., 2000] to identify the effective conductivities of the three tissue layers. In MEG, inaccuracy in conductivity values is a minor concern [Hämäläinen and Sarvas, 1989], whereas in EEG, inaccuracies in the skull conductivity may significantly contribute to forward computation errors [Cohen and Cuffin, 1983; de Jongh et al., 2005; Okada et al., 1999b; Tarkiainen et al., 2003]. Since our noise estimates were either computed from the measured data or matched to the experimental sensor variances, the effect of the conductivity uncertainties on the noise estimates was minor. Recalculating the noise source variance without EEG, on average the difference in s_s was less than 5% compared with the calculation that included EEG. This suggests that the uncertainty in the conductivity values had only little effect on the estimated noise source variance. However, if the true conductivity of the skull is higher or lower than that used in our forward model, our EEG SNR estimates are too large or too small, respectively.

We computed the average SNR across channels [Fuchs et al., 1998], rather than the maximum value of SNR [de Jongh et al., 2005]. The average and maximum SNR values will be more similar for widespread than for focal signal patterns. Therefore, our use of the average SNR is likely to bias the difference SNR maps towards larger relative values for EEG compared with MEG. It is important to take

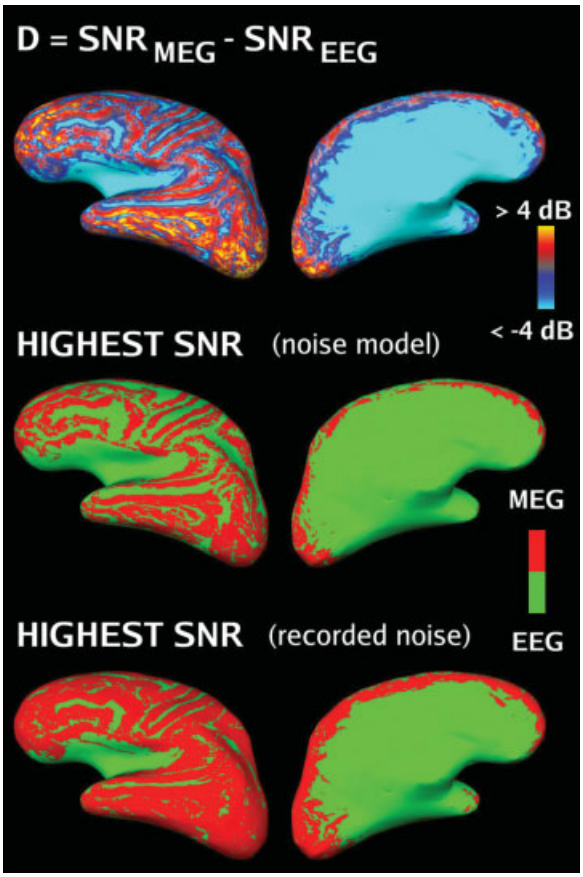

Figure 3.

Difference (D) SNR maps (group average, left hemisphere, plotted on the brain of Subject 2). Top row: Difference (D) maps based on the noise model. Middle row: D maps based on the noise model thresholded at $D = 0$. Red: $D > 0$ (MEG higher SNR), green: $D < 0$ (EEG higher SNR). The sulci, narrow crests of gyri, the insula and the medial surface of the cortex all indicate higher SNR in EEG, while other locations show higher SNR in MEG. Bottom row: D maps based on recorded noise thresholded at $D = 0$.

this into account when comparing the SNR across different sensor types. For example, differential recordings, such as bipolar EEG or gradiometric MEG have a more spatially focal signal pattern compared with the average reference EEG or magnetometric MEG, respectively. We chose the average SNR because this measure appears more relevant to the application of source localization techniques which generally benefit from several sensors exhibiting a high SNR.

Previous studies matched the number and locations of EEG electrodes and MEG sensors [Fuchs et al., 1998; Liu et al., 2002]. In contrast, we compared a 306-channel MEG system to a 70-channel EEG system, both of which are currently used in clinical studies of epileptic patients in our laboratory. There is evidence to suggest that these provide sufficient spatial sampling [Ahonen et al., 1993; Grieve et al., 2004; Lantz et al., 2003]; therefore, the exact quantity and position of channels is expected to have little effect on the SNR maps.

To examine general features of the SNR maps, we used a noise model that only accounted for the contributions of uniformly distributed cortical noise sources, excluding instrumentation and environmental noise. In practice, however, it is preferable to use session-specific noise esti-

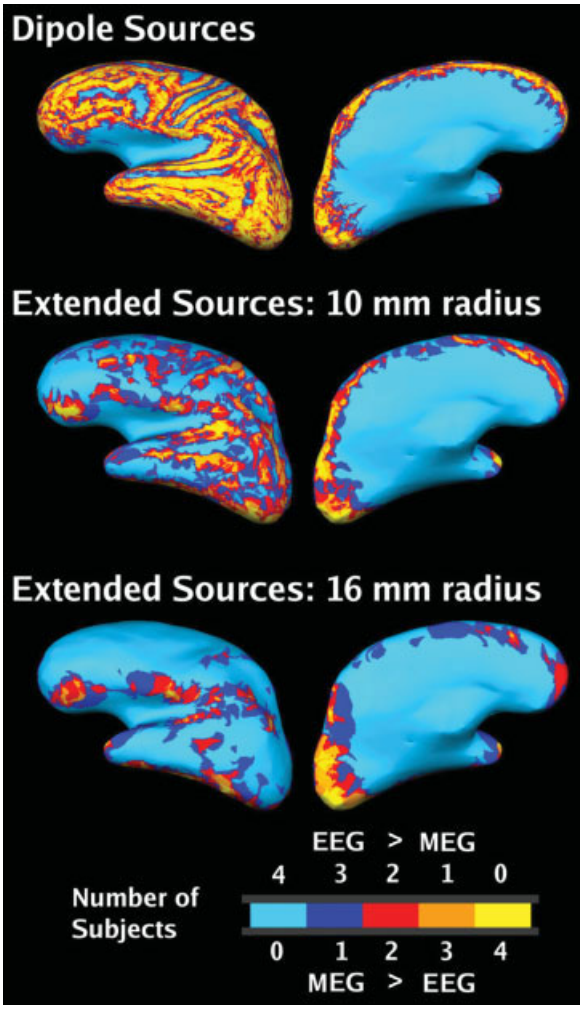

Figure 4.

Effect of the extent of the source on SNR maps (noise model, group average, left hemisphere, plotted on subject 2's brain). Top row: Dipoles. Middle row: Extended patch sources, radius = 10 mm. Lower row: Extended patch sources, radius = 16 mm. The color code indicates at each location the number of subjects that have $SNR_{MEG} > SNR_{EEG}$ (i.e. $D > 0$). For example, areas colored yellow exhibited $D > 0$ in all four subjects at that location. The intermediate colors indicate locations with greater between-subject variability.

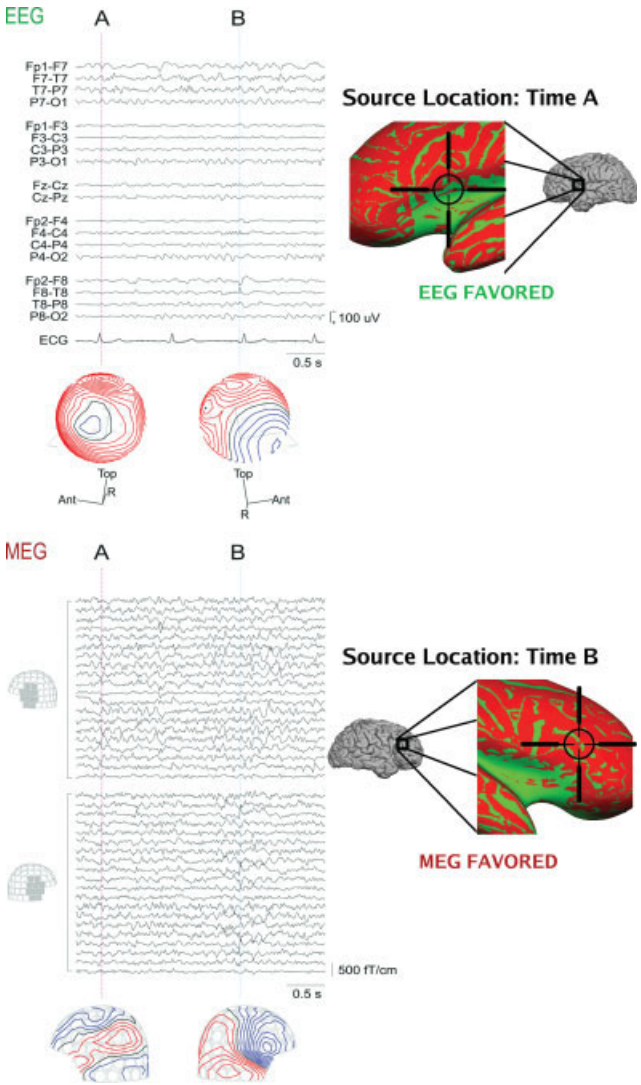

Figure 5.

MEG and EEG recording from an epileptic patient. Left, above: The EEG signals (standard clinical bipolar montage) and potential distributions at time instants A and B. Left, below: MEG signals in left and right frontotemporal planar gradiometers and the corresponding field distributions at times A and B. The spike at time A can be more easily detected from the EEG data whereas the spike at time B is more prominent in the MEG signals. Right: The locations of the spike sources at times A and B estimated with an equivalent current-dipole model are superimposed on the difference SNR maps (green: $SNR_{EEG} > SNR_{MEG}$, red: $SNR_{MEG} > SNR_{EEG}$). Pial cortex maps are shown as well as expanded SNR maps in the region of the dipole source. The SNR maps correctly identify the modality that best represents the spikes at times A and B respectively.

mated from recorded data. The difference between the results obtained with the noise model and the recorded noise may be in part due to the fact that intrinsic background brain activity from focal sources is detected in a greater number of sensors in EEG than in MEG; therefore, regional sources (such as the alpha rhythm) have a spatial distribution that is more similar to that of a widely distributed noise source in EEG than it is in MEG. The eye blink, muscle movement, and cardiac artifacts were not included because they are of transient rather than random nature and can be either excluded from the data analysis or dampened by noise rejection techniques.

MEG and EEG

The SNR maps indicated complementary properties for MEG and EEG across the cortical surface, suggesting that combined recordings can be beneficial. The SNR of deeper sources, including those in the medial cortex and the insula, was larger in EEG, whereas the SNR of more superficial sources was often larger in MEG. Additionally, locations with source orientations normal to the inner skull surface (i.e., radial dipoles), such as the crests of gyri, are difficult to detect with MEG [Barkley and Baumgartner, 2003; Cohen, 1972; Cuffin and Cohen, 1979; Hämäläinen et al., 1993; Melcher and Cohen, 1988; Pataraia et al., 2002]. However, the attenuation of MEG SNR due to orientation is relevant to only ~5% of the cortical surface [Hillebrand and Barnes, 2002]; the majority of the differences can be accounted for by depth considerations.

Our results are consistent with previous studies where regional differences in MEG and EEG have been observed. Several studies have reported that MEG is not well suited for mesial temporal lobe epilepsy [Baumgartner et al., 2000; de Jongh et al., 2005; Leitjen et al., 2003; Lin et al., 2003; Shigeto et al., 2002]. Conversely, it has been noted that MEG can improve the diagnostic yield for sources in the lateral aspect of the temporal lobe [Baumgartner et al., 2000; de Jongh et al., 2005; Leitjen et al., 2003] and in frontal regions [de Jongh et al., 2005; Ossenblok et al., 1999]. It is important to note, however, that the MEG SNR may be critically affected by the positioning of the sensor array with respect to the head; in particular, large differences in signals from frontal sources have been demonstrated [Marinkovic et al., 2004].

The SNR maps also help to better understand why sometimes certain epileptic spikes are detected only in one modality but not the other [Baumgartner et al., 2000; Iwasaki et al., 2005; Knake et al., 2006; Leitjen et al., 2003; Lin et al., 2003; Yoshinaga et al., 2002; Zijlmans et al., 2002]. In particular, as the sources that generate an MEG signal are, theoretically, only a subset (nonradial, superficial) of the sources that generate an EEG signal, it can be counter-intuitive that spikes are detected in MEG but not in EEG. However, not only the amplitude of the activity, but also the magnitude of noise affects the detectability of spikes in MEG and EEG. Indeed, signals that have been detected in one modality may also be identified in the other modality, but with low SNR [Yoshinaga et al., 2002, Zijlmans et al., 2002]. Our patient data also demonstrated this.

The SNR maps indicated that as the source extent grew from a dipole to extended sources of radius 10 mm (area = 3 cm^2) and 16 mm (8 cm^2), the number of locations with $SNR_{MEG} > SNR_{EEG}$ diminished. This is likely to reflect selective cancellation of signals from the tangential source components [Eulitz et al., 1997]. In our simulations we only varied the extent of the signal source, but kept the noise model unchanged. Therefore, the same trend towards larger relative SNR values for EEG compared with MEG would also be found with actual recorded noise (which is independent of the source model). However, if extended source patches were included in the noise model, this would be expected to compensate for the changes in the difference SNR maps, thereby increasing the relative SNR of MEG compared with EEG.

In general, if one assumes that the source density is approximately constant [Lu and Willamson, 1991], a larger patch is expected to result in larger signals, thereby increasing the SNR. Our SNR maps for extended sources are consistent with previous reports of the size of activated are of cortex underlying detectable EEG and MEG signals. By some estimates, 6–10 cm^2 of cortex must be active for EEG to detect signals at the scalp [Ebersole and Pedley, 2002; Nunez, 1990]. A combined MEG and intracranial electrode study [Baumgartner et al., 2000] stated that a 4 cm^2 patch of cortex was invisible to MEG on the mesial temporal lobe, while an 8 cm^2 one was visible. In our study, 3 cm^2 (radius 10 mm) sources had a 10 dB lower SNR than the 8 cm^2 (radius 16 mm) sources in the mesial temporal lobe. However, the variability across cortical locations was large; for example, the difference between 3 cm^2 and the 8 cm^2 sources in the EEG SNR ranged from less than 1 dB to more than 10 dB. Therefore, it is important to consider not only the extent but also the anatomical location when assessing the detectability of cortical activation.

Clinical Implications

The results of this study have practical consequences in the clinical evaluation of patients with epilepsy prior to surgery. Because optimized localization results in better surgical outcome [Ebersole and Pedley, 2002; Stefan et al., 2003], seizure focus localization should be performed with the modality having the highest SNR for the given position. In addition, it can be employed to test that the head position was appropriate during a MEG recording. The SNR values critically depend on head position [Marinkovic et al., 2004], therefore any focal source identified in unexpected cortical regions (such as an occipital focus identified when searching for a frontal focus) should be checked for high enough SNR to be considered reliable. Similarly, the SNR maps can be used as a more general marker of reliability – thus source positions with very low SNR cannot be considered as accurately localized as sources with high SNR. When noise is high, spurious signals could result in greater mis-localization for regions with low SNR, such as in deep cortical structures.

It is possible that a method for a combined MEG and EEG inverse model can be achieved by examining the SNR at each sensor. It could weigh channels from simultaneously collected MEG/EEG data on the basis of SNR per channel. Such a combined inverse model may improve the accuracy because estimates will rely on channels more directly affected by modeled sources. Patients who undergo MEG for presurgical evaluation routinely obtain simultaneous EEG; therefore, data for such a combined inverse solution would be easy to implement and could improve localizations.

Furthermore, we believe that knowledge of the SNR values for various cortical regions may be beneficial in the development of a more statistically rigorous source estimation technique for epileptic focus evaluation. Such an algorithm would use the reliability index from the SNR maps as well as the more traditional measures of error. The result would be a more clinically based test—one that could clarify the relative importance of an EEG/MEG source localization in the context of other imaging modalities (MRI, positron emission tomography, single photon emission computed tomography, functional MRI, etc) by assigning a probability of accuracy to source estimates.

CONCLUSIONS

The SNR maps were complementary for EEG and MEG, displaying regional differences among sources within the cortical surface. The noise model based only on uniform background brain activity was found to underestimate the SNR in MEG. With extended sources, the total area of cortex in which the SNR was higher in EEG than in MEG was larger than that with focal sources. The SNR maps help to better understand why epileptic activity is in some cases detected in one modality (EEG or MEG) only. The results suggest that combing EEG and MEG recordings is beneficial. In addition, there may be clinical utility to using SNR maps when evaluating patients with epilepsy presurgically both in order to optimize the localization and to put MEG/EEG localization in context with other structural and functional imaging modalities.

ACKNOWLEDGMENTS

We thank Deirdre Foxe and Daniel Wakeman for technical assistance.

REFERENCES

Ahonen AI, Hämäläinen MS, Ilmoniemi RJ, Kajola MJ, Knuutila JE, Simola JT, Vilkman VA (1993): Sampling theory for neuromagnetic detector arrays. IEEE Trans Biomed Eng 40:859–869.

Babiloni F, Babiloni C, Carducci F, Romani GL, Rossini PM, Angelone LM, Cincotti F (2004): Multimodal integration of EEG and MEG data: a simulation study with variable signal-to-noise ratio and number of sensors. Hum Brain Mapp 22:52–62.

Barkley GL, Baumgartner C (2003): MEG and EEG in epilepsy. J Clin Neurophysiol 20:163–178.

Baumgartner C (2004): Controversies in clinical neurophysiology. MEG is superior to EEG in the localization of interictal epileptiform activity: Con. Clin Neurophysiol 115:1010–1020.

Baumgartner C, Pataraia E, Lindinger G, Deecke L (2000): Neuromagnetic recordings in temporal lobe epilepsy. J Clin Neurophysiol 17:177–189.

Cobb WA, editor (1983): IFCN Recommendations For The Practice Of Clinical Neurophysiology. Amsterdam: Elsevier.

Cohen D (1972): Magnetoencephalography: Detection of the brain's electrical activity with a superconducting magnetometer. Science 175:664–666.

Cohen D, Cuffin BN (1983): Demonstration of useful differences between magnetoencephalogram and electroencephalogram. Electroencephalogr Clin Neurophysiol 56:38–51.

Cohen D, Cuffin BN, Yunokuchi K, Maniewski R, Purcell C, Cosgrove GR, Ives J, Kennedy JG, Schomer DL (1990): MEG versus EEG localization test using implanted sources in the human brain. Ann Neurol 28:811–817.

Crouzeix A, Yvert B, Bertrand O, Pernier J (1999): An evaluation of dipole reconstruction accuracy with spherical and realistic head models in MEG. Clin Neurophysiol 110:2176–2188.

Cuffin BN, Cohen D (1979): Comparison of the magnetoencephalogram and electroencephalogram. Electroencephalogr Clin Neurophysiol 47:132–146.

Dale AM, Fischl B, Sereno MI (1999): Cortical surface-based analysis. I. Segmentation and surface reconstruction Neuroimage 9:179–194.

de Jongh A, de Munck JC, Goncalves SI, Ossenblok P (2005): Differences in MEG/EEG epileptic spike yields explained by regional differences in signal-to-noise ratios. J Clin Neurophysiol 22:153–158.

de Munck JC, Vijn PC, Lopes da Silva FH (1992): A random dipole model for spontaneous brain activity. IEEE Trans Biomed Eng 39:791–804.

Dijkstra EW (1959): A note on two problems in connection with graphs. Numeriche Mathematik 1,269–271.

Ebersole JS, Pedley TA, editors (2002): Current Practice of Clinical Electroenchalography. Philadelphia: Lippincott Williams & Wilkins. p 974.

Eulitz C, Eulitz H, Elbert T (1997): Differential outcomes from magneto-and electroencephalography for the analysis of human cognition. Neurosci Lett 227:185–188.

Fischl B, Sereno MI, Dale AM (1999a) Cortical surface-based analysis. II: Inflation, flattening, and a surface-based coordinate system. Neuroimage 9:195–207.

Fischl B, Sereno MI, Tootell RB, Dale AM (1999b) High-resolution intersubject averaging and a coordinate system for the cortical surface. Hum Brain Mapp 8:272–284.

Fischl B, Liu A, Dale AM (2001): Automated manifold surgery: Constructing geometrically accurate and topologically correct models of the human cerebral cortex. IEEE Trans Med Imaging 20:70–80.

Fuchs M, Wagner M, Wischmann HA, Kohler T, Theissen A, Drenckhahn R, Buchner H (1998): Improving source reconstructions by combining bioelectric and biomagnetic data. Electroencephalogr Clin Neurophysiol 107:93–111.

Fuchs M, Wagner M, Kastner J (2001): Boundary element method volume conductor models for EEG source reconstruction. Clin Neurophysiol 112:1400–1407.

Goncalves S, de Munck JC, Heethaar RM, Lopes da Silva FH, van Dijk BW (2000): The application of electrical impedance tomography to reduce systematic errors in the EEG inverse problem–a simulation study. Physiol Meas 21:379–393.

Grieve PG, Emerson RG, Isler JR, Stark RI (2004): Quantitative analysis of spatial sampling error in the infant and adult electroencephalogram. Neuroimage 21:1260–1274.

Hämäläinen MS, Sarvas J (1989): Realistic conductivity geometry model of the human head for interpretation of neuromagnetic data. IEEE Trans Biomed Eng 36:165–171.

Hämäläinen MS, Hari R, Ilmoniemi RJ, Knuutila J, Lounasmaa O (1993): Magnetoencephalography-theory, instrumentation, and applications to noninvasive studies of the working human brain. Rev Modern Phys 65:1–93.

Hillebrand A, Barnes GR (2002): A quantitative assessment of the sensitivity of whole-head MEG to activity in the adult human cortex. Neuroimage 16:638–650.

Iwasaki M, Pestana E, Burgess RC, Luders HO, Shamoto H, Nakasato N (2005): Detection of epileptiform activity by human interpreters: Blinded comparison between electroencephalography and magnetoencephalography. Epilepsia 46:59–68.

Knake S, Halgren E, Shiraishi H, Hara K, Hamer HM, Grant PE, Carr VA, Foxe D, Camposano S, Busa E, Witzel T, Hämäläinen MS, Ahlfors SP, Bromfield EB, Black PM, Bourgeois BF, Cole AJ, Cosgrove GR, Dworetzky BA, Madsen JR, Larsson PG, Schomer DL, Thiele EA, Dale AM, Rosen BR, Stufflebeam SM (2006): The value of multichannel MEG and EEG in the presurgical evaluation of 70 epilepsy patients. Epilepsy Res 69:80–86.

Lantz G, Grave de Peralta R, Spinelli L, Seeck M, Michel CM (2003): Epileptic source localization with high density EEG: How many electrodes are needed? Clin Neurophysiol 114:63–69.

Leahy RM, Mosher JC, Spencer ME, Huang MX, Lewine JD (1998): A study of dipole localization accuracy for MEG and EEG using a human skull phantom. Electroencephalogr Clin Neurophysiol 107:159–173.

Leijten FS, Huiskamp GJ, Hilgersom I, Van Huffelen AC (2003): High-resolution source imaging in mesiotemporal lobe epilepsy: a comparison between MEG and simultaneous EEG. J Clin Neurophysiol 20:227–238.

Lesser RP (2004): MEG: Good enough. Clin Neurophysiol 115:995–997.

Lin YY, Shih YH, Hsieh JC, Yu HY, Yiu CH, Wong TT, Yeh TC, Kwan SY, Ho LT, Yen DJ, Wu ZA, Chang MS (2003): Magnetoencephalographic yield of interictal spikes in temporal lobe epilepsy. Comparison with scalp EEG recordings. Neuroimage 19:1115–1126.

Liu AK, Dale AM, Belliveau JW (2002): Monte Carlo simulation studies of EEG and MEG localization accuracy. Hum Brain Mapp 16:47–62.

Lopes da Silva FH, Wieringa HJ, Peters MJ (1991): Source localization of EEG versus MEG: Empirical comparison using visually evoked responses and theoretical considerations. Brain Topogr 4:133–142.

Lu ZL, Williamson SJ (1991): Spatial extent of coherent sensory-evoked cortical activity. Exp Brain Res 84:411–416.

Marinkovic K, Cox B, Reid K, Halgren E (2004): Head position in the MEG helmet affects the sensitivity to anterior sources. Neurol Clin Neurophysiol 30:30.

Melcher JR, Cohen D (1988): Dependence of the MEG on dipole orientation in the rabbit head. Electroencephalogr Clin Neurophysiol 70:460–472.

Nunez PL (1990): Localization of brain activity with electroencephalography. In: Sato S, editor. Advances in Neurology, Vol. 54. Magnetoencephalography. New York: Raven Press. pp 39–65.

Okada Y, Lahteenmaki A, Xu C (1999b) Comparison of MEG and EEG on the basis of somatic evoked responses elicited by stimulation of the snout in the juvenile swine. Clin Neurophysiol 110:214–229.

Ossenblok P, Fuchs M, Velis DN, Veltman E, Pijn JP, da Silva FH (1999): Source analysis of lesional frontal-lobe epilepsy. IEEE Eng Med Biol Mag 18:67–77.

Pataraia E, Baumgartner C, Lindinger G, Deecke L (2002): Magnetoencephalography in presurgical epilepsy evaluation. Neurosurg Rev 25:141–159; discussion 160–161.

Pataraia E, Lindinger G, Deecke L, Mayer D, Baumgartner C (2005): Combined MEG/EEG analysis of the interictal spike complex in mesial temporal lobe epilepsy. Neuroimage 24:607–614.

Segonne F, Dale AM, Busa E, Glessner M, Salat D, Hahn HK, Fischl B (2004): A hybrid approach to the skull stripping problem in MRI. Neuroimage 22:1060–1075.

Shigeto H, Morioka T, Hisada K, Nishio S, Ishibashi H, Kira D, Tobimatsu S, Kato M (2002): Feasibility and limitations of magnetoencephalographic detection of epileptic discharges: Simultaneous recording of magnetic fields and electrocorticography. Neurol Res 24:531–536.

Stefan H, Hummel C, Scheler G, Genow A, Druschky K, Tilz C, Kaltenhauser M, Hopfengartner R, Buchfelder M, Romstock J (2003): Magnetic brain source imaging of focal epileptic activity: a synopsis of 455 cases. Brain 126:2396–2405.

Tarkiainen A, Liljeström M, Seppä M, Salmelin R (2003): The 3D topography of MEG source localization accuracy: Effects of conductor model and noise. Clin Neurophysiol 114:1977–1992.

Tesche CD, Uusitalo MA, Ilmoniemi RJ, Huotilainen M, Kajola M, Salonen O (1995): Signal-space projections of MEG data characterize both distributed and well-localized neuronal sources. Electroencephalogr Clin Neurophysiol 95:189–200.

Wiebe S, Blume WT, Girvin JP, Eliasziw M (2001): A randomized, controlled trial of surgery for temporal-lobe epilepsy. N Engl J Med 345:311–318.

Wood CC, Cohen D, Cuffin BN, Yarita M, Allison T (1985): Electrical sources in human somatosensory cortex: Identification by combined magnetic and potential recordings. Science 227:1051–1053.

Yoshinaga H, Nakahori T, Ohtsuka Y, Oka E, Kitamura Y, Kiriyama H, Kinugasa K, Miyamoto K, Hoshida T (2002): Benefit of simultaneous recording of EEG and MEG in dipole localization. Epilepsia 43:924–928.

Zijlmans M, Huiskamp GM, Leijten FS, Van Der Meij WM, Wieneke G, Van Huffelen AC (2002): Modality-specific spike identification in simultaneous magnetoencephalography/electroencephalography: A methodological approach. J Clin Neurophysiol 19:183–191.